

Computed tomography and laser scanning of fossil cephalopods (Triassic and Cretaceous)

A. LUKENEDER, S. LUKENEDER & C. GUSENBAUER

Abstract: We here present a computed tomography and 3D visualisation of Mesozoic cephalopods from the Southern Alps and the Taurus Mountains. Study objects were ammonoids and ammonoid mass-occurrences that were deposited during the Upper Triassic (approx. 234 mya) of SW Turkey and during the Lower Cretaceous of N Italy (approx. 129 mya). Computed tomography, a non-destructive and non-invasive method, facilitates the view inside rocks and fossils. The combination of computed tomography and palaeontological data enable us to produce 3D reconstructions of the extinct organisms. Detailed reconstructions of the fossil cephalopods and the ammonite animals are based on shell morphologies, adapted from CT data. Object-based combined analyses from computed tomography and various computed 3D facility programmes aid in understanding morphological details as well as their ontogenetic changes in fossil material. The presented CT and laser scan data demonstrate the wide range of applications and analytical techniques, and furthermore outline possible limitations of computed tomography in earth sciences and palaeontology.

Keywords: Computed tomography, laser scan, palaeontology, ammonoids, Triassic, Cretaceous

Introduction

X-ray computed tomography and laser scanning is known in palaeontology as providing data for 3D visualisation and geometrical modelling techniques. Computed tomography and laser scans down to a few microns (or even below) of spatial resolution are increasingly employed for geoscientific investigations, using an equally variable range of processing techniques and software packages. Additionally, internal structures are visualised without the destruction of fossils, as computed tomography is a non-destructive method.

The creation of 3D models from fossils (e.g. cephalopods) based on CT and laser scan imaging aids in visualisation and interpretation, and may serve for the reconstruction of mechanical models. 3D models of fossil specimens have become increasingly popular, providing more or less accurate information about volume, spatial distribution, orientation and size of fossils in a sample as well as insights into biostratigraphic and diagenetic processes. Numerous complementary techniques have been advanced in recent years. These provide 3D datasets of palaeontological objects and involve both surface and volume scanning methods (e.g. microtomography), as well as laser scanning (airborne, terrestrial or desktop scanners) of surface morphology. These methods can be combined with point cloud data generated from digital images. Numerous authors (e.g. MARSCHALLINGER 2001; MALOOF et al. 2010;

MAYRHOFFER & LUKENEDER 2010; KRUTA et al. 2011; MARSCHALLINGER et al. 2011; LUKENEDER S. & A. LUKENEDER 2011; SAUPE et al. 2012) show the multitude of applications of 3D geometrical models in palaeontological studies. The great variability, the wide range of applications, and the analytical techniques in the fossil record are demonstrated for dinosaurs (RAYFIELD et al. 2001, 2007; BALANOFF et al. 2008; WITMER and RIDGELY 2009; FORTUNY et al. 2011; TSUIHJI et al. 2011; KNOLL et al. 2012), lizards (POLCYN et al. 2002), birds (ROWE et al. 2001; DEGRANGE et al. 2010; ZELENITSKY et al. 2011), fishes (GAI et al. 2011), mammals (LUO et al. 2002), molluscs (HOFFMANN & ZACHOW 2011; LUKENEDER A. 2012; LUKENEDER A. et al. 2012, 2014), brachiopods (GASPARD et al. 2011), insects (GARWOOD 2010, 2011; GARWOOD et al. 2009), plants (FRIIS et al. 2007; SCOTT et al. 2009; LUKENEDER A. et al. 2012), algal or acritarch fossils (CUNNINGHAM et al. 2012), and protists (DONOGHUE et al. 2006, DONG et al. 2010; HULDTGREN et al. 2011). The latter papers additionally outline possible limitations of 3D models in earth sciences and in palaeontology.

The main goal of this paper is to present methods and possibilities for visualisation of palaeontological material based on computed tomography, laser scanning and palaeontological features (e.g. morphology; Fig. 1). Case studies on computed tomography within two 3-year projects of the Austrian Science Fund (FWF

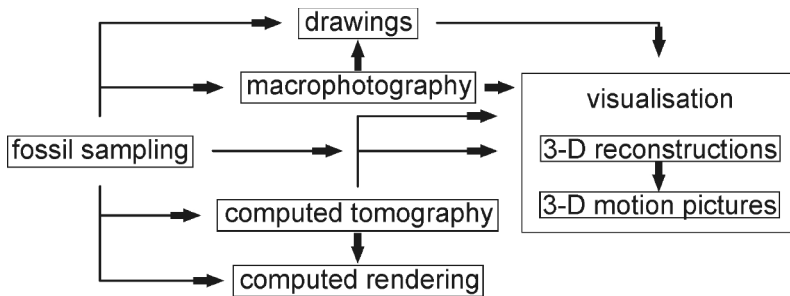


Fig. 1: Principal steps in 3D visualisation of palaeontological material such as ammonoids.

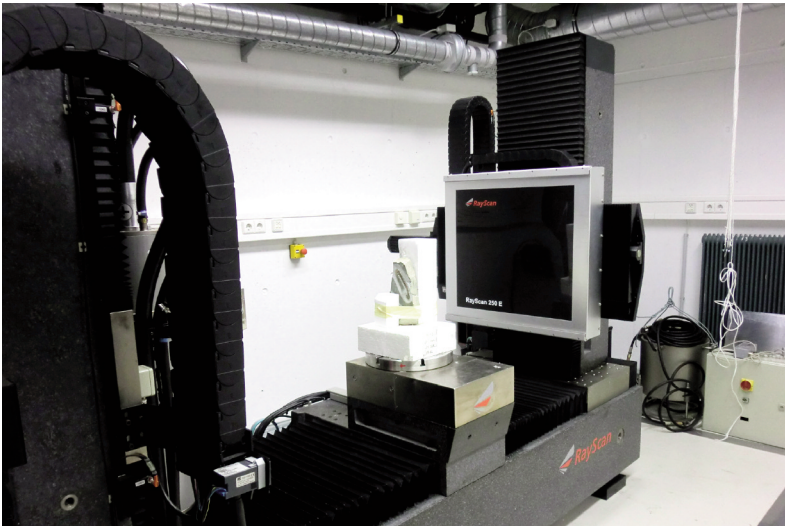


Fig. 2: The CT RayScan 250 E device, with a 225 kV micro-focus and with a 450 kV mini-focus X-ray tube and a 2048 × 2048 pixel flat panel detector (cone beam reconstruction) located at the University of Applied Sciences Upper Austria, Wels Campus. Note the fixed limestone sample with the Lower Cretaceous ammonite *Dissimilites* in the centre.

P22109-B17 and P20018-N10) on Triassic and Cretaceous ammonoids can demonstrate the increasing importance of CT and laser scanning methods in palaeontology.

Experimental design of computed tomography and laser scanning

Computed tomography

Non-invasive techniques, e.g. computed tomography, allow to process great volumes of information without causing any alteration of fossil material (LUKENEDER A. 2012; LUKENEDER A. et al. 2014). The tomography scans used within this study were made at the Upper Austria University of Applied Sciences in Wels. The 3D computed tomography (CT) device RayScan 250 E is a 3D CT system equipped with two X-ray sources (a 225 kV micro-focus and a 450 kV mini-focus X-ray tube) for the inspection of a wide variety of parts, ranging from micro-objects (high resolution) to macroscopic ones

(large penetration length). The system is additionally equipped with a 2048 × 2048 pixels flat-panel detector; it absorbs energy of the X-rays and re-emits the absorbed energy in the form of light, which can be detected (Fig. 2). In the case of an industrial CT-system, the specimen is rotated by 360° and at each predefined angle step a 2D-projection image is captured. The complete set of projection images is then reconstructed to 3D volume data using a mathematical algorithm. The data consists of volumetric pixels (voxels), whose size limits the spatial resolution (down to 5 μm) and the detail-detectability. For each fossil part, the optimal voxel size and tube voltage were set according to the specimen's dimensions. A more detailed introduction to computed tomography is beyond the scope of this article. For the details of X-ray computed tomography as a technique of imaging and quantification of internal features of sediments and fossils see MEES et al. (2003). The non-destructive CT provides the basal information on morphological features of the respective fossil cephalopods.

Laser scanning

Laser scanning of surface morphology is increasingly employed for geoscientific investigations, using an equally variable range of processing techniques and software packages. By using laser surface scans, individual statistical information (e.g. length, breadth, diameter) can be measured very fast and accurately without destruction of the fossil material. Statistical analyses can be performed much quicker and occasionally even more precise in digital systems (LUKENEDER S. & A. LUKENEDER 2011). For instance, surface scans of single ammonoids of the genus *Kasimlarceltites* (with 99.9% the dominant species of the Triassic ammonoid mass-occurrence) can be used for reconstructing *Kasimlarceltites* as close as possible to nature (Fig. 10a, b). Therefore 3D surface laser scan data were produced down to a resolution of 0.25 mm by using a FARO® Laser Scanner Photon 120/20 and visualised with a new software-version FARO Scene 4.6. The software package 3D-Tool V8 was used for creating digital-slices of single ammonoids (Fig. 10e) and processing size, orientation and distribution of the ammonoids within the mass occurrence (Fig. 10f–h). 3D laser scans and their visualisation were made in cooperation with the Department of Geodynamic and Industrial Geometry Group (3D technology at the University of Technology Vienna) and the Lower Austrian government agency for Hydrogeology and Geoinformation.

The new FARO® Laser Scanner Photon 120/20, with the new software-version FARO Scene 4.6, possesses the fastest Phase Shift Laser Scanner (976.000 points/seconds) with the biggest range that is currently

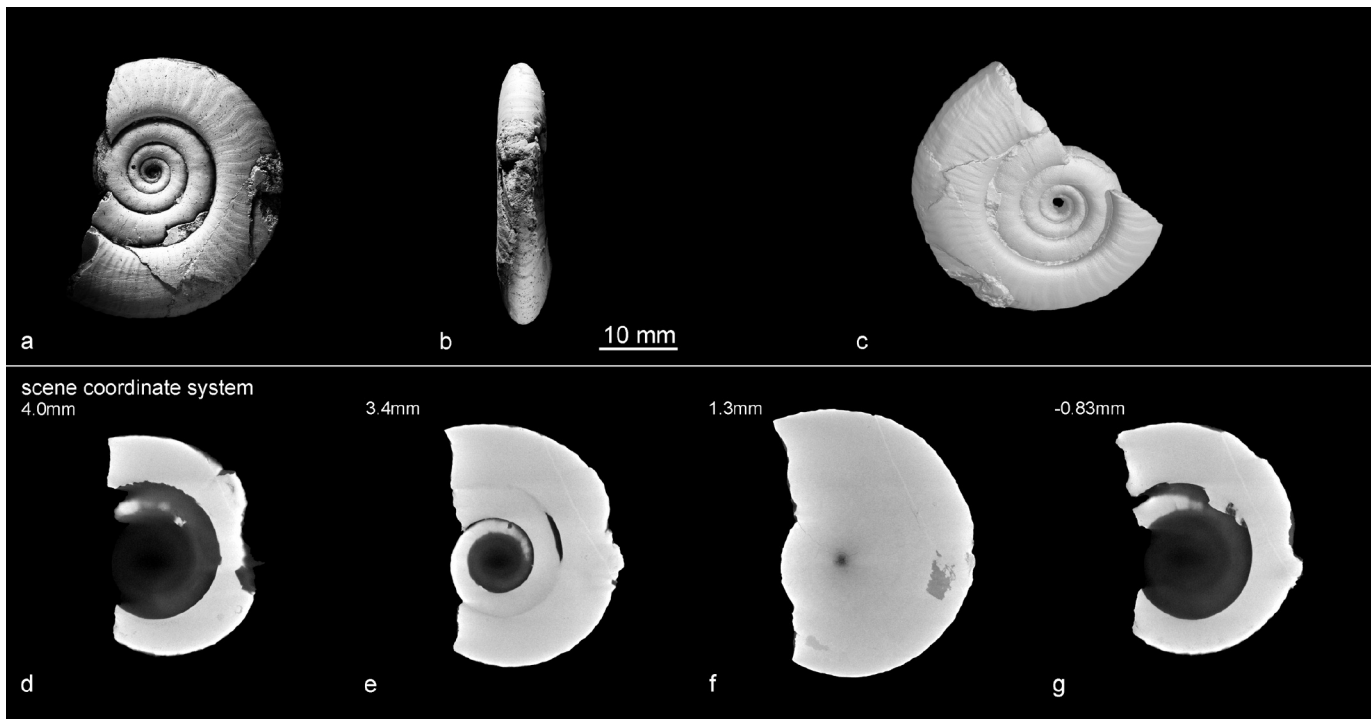


Fig. 3: *Kasimlarceltites krystyni*. (a) Lateral view; (b) ventral view of the holotype, NHMW-2012z0133/0014, both coated with ammonium chloride; (c) rendered CT surface of the same specimen. CT frontal view slices: (d) CT slice 048; (e) CT slice 076; (f) CT slice 168; (g) CT slice 260. Embedding and infilling sediment is limestone.

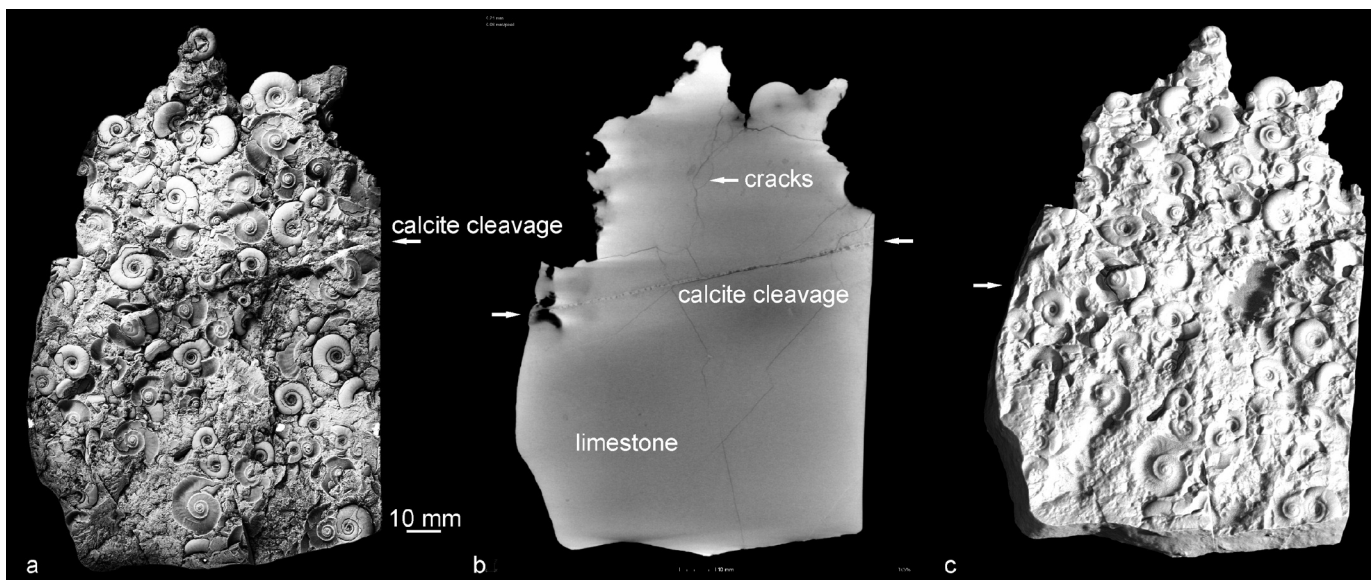


Fig. 4: Rock sample with the mass-occurrence of *Kasimlarceltites krystyni*. (a) Lateral view, NHMW-2013/0568/0003, coated with ammonium chloride; (b) CT frontal view slice 733; (c) rendered CT surface of the same sample. Embedding and infilling sediment is limestone. Note the visible cleavage and cracks.

available on the free market. New technical features of the Photon 120/20 make the scanner a useful system for performing high-speed 3D scans with reduced random-noise obtained by efficient hyper-modulation. Surfaces of ammonoids can therefore be reconstructed digitally without loss of information.

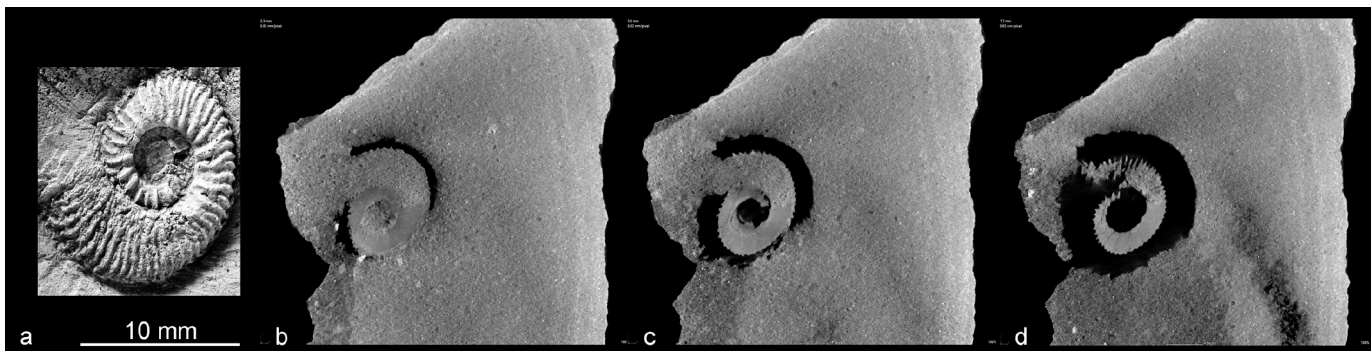


Fig. 5: *Sandlingites* cf. *pilari*. (a) Lateral view, NHMW-2012/0133/0475, coated with ammonium chloride. CT frontal view slices: (b) CT slice 185; (c) CT slice 199; (d) CT slice 215. Spotty grey, embedding sediment and infilling of body chamber is sandstone. Smooth grey, internal parts filled by secondary calcite in the phragmocone.

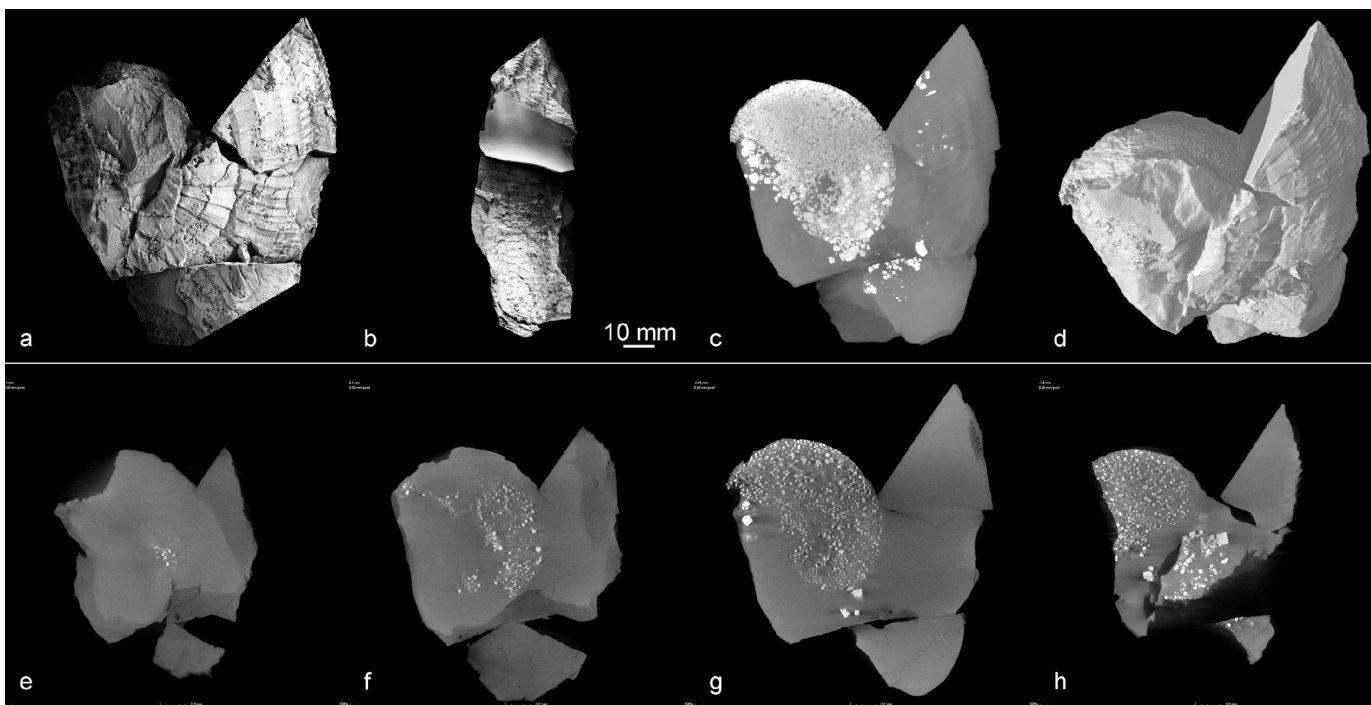


Fig. 6: *Trachysagenites* cf. *beckei*. (a) Lateral view, NHMW-2012/0133/0350; (b) ventral view, coated with ammonium chloride; (c) maximum intensity projection; (d) rendered CT surface of the same specimen. CT frontal view slices: (e) CT slice 095; (f) CT slice 144; (g) CT slice 295; (h) CT slice 418. Embedding and infilling sediment is limestone. Note the numerous whitish pyrite cubes in the phragmocone.

Palaeontological material

Triassic ammonoids from the Taurus Mountains in Turkey

Computed tomography was tested on the Triassic ammonoid genera *Kasimlarceltites* (and its mass-occurrence), *Sandlingites* and *Trachysagenites*. These fossil cephalopods originate from the Upper Triassic (Carnian, approx. 234 mya) Aşağıyaylabel locality (Taurus Mountains, southwest Turkey). The material was collected within the FWF project P22109-B17 and is stored at the Natural History Museum in Vienna (NHMW). Inventory numbers are given for the investigated specimens of *Kasimlarceltites* (holotype NHMW-

2012/0133/0014), *Sandlingites* (NHMW-2012/0133/0475) and *Trachysagenites* (NHMW-2012/0133/0350). The ammonoids were collected by Alexander and Susanne LUKENEDER, Andreas GINDL, Mathias HARZHAUSER, Leopold KRISTYN, Philipp STRAUSS, and Franz TOPKA.

The outcrop at Aşağıyaylabel is situated at steep limestone walls (dipping 50 degrees NE) within the Taurus Mountains of southern Turkey (Anatolia), about 90 km NNE of Antalya, between the lakes Egirdir and Beyshehir (GPS coordinates N37°33'05" E31°18'14"; LUKENEDER S. & A. LUKENEDER 2014). The fossil cephalopods reported within this work derive from the

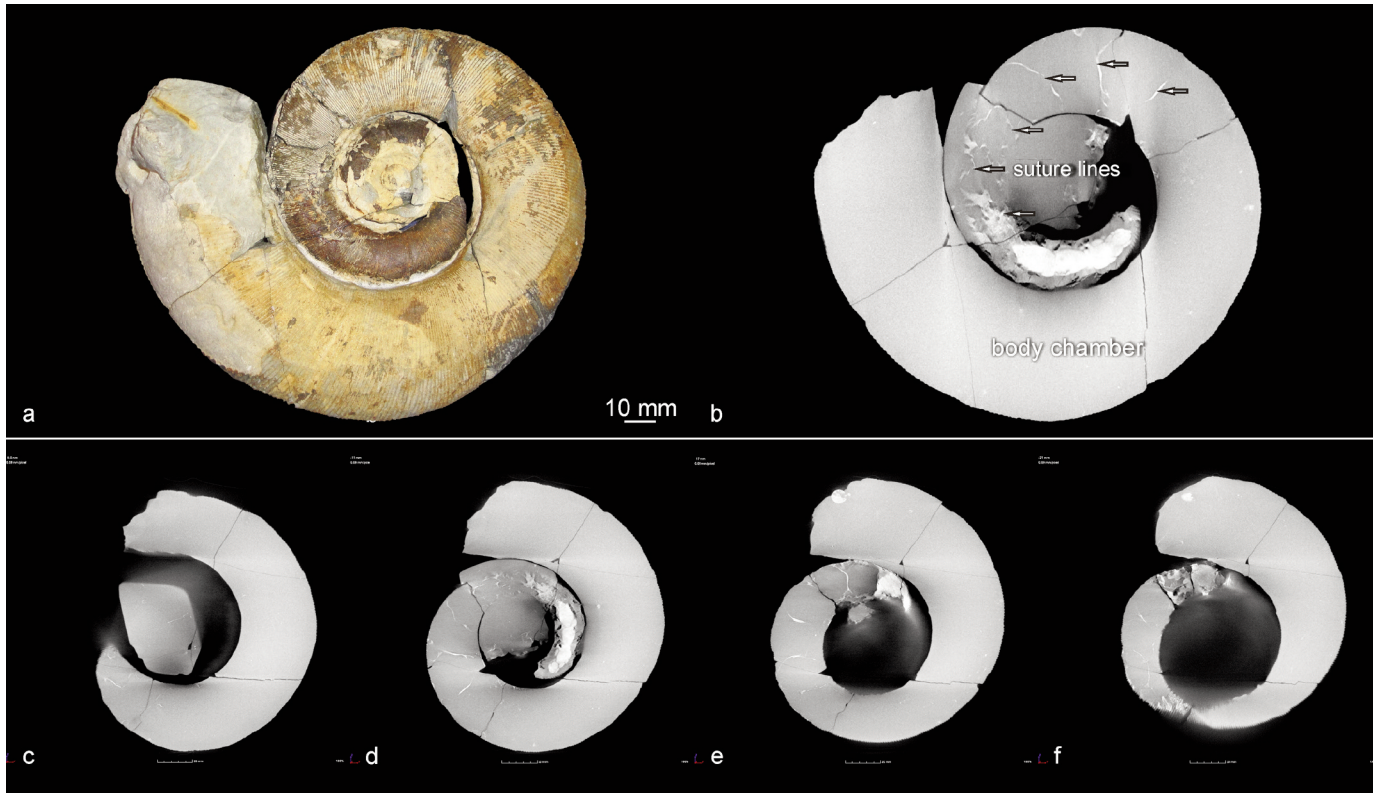


Fig. 7: *Lytoceras subfimbriatum*. (a) Lateral view, uncoated with yellow limonitic crust, NHMW- 2013/0569/0001; (b) maximum intensity projection. CT frontal view slices: (c) CT slice 186; (d) CT slice 252; (e) CT slice 317; (f) CT slice 351. Note the visible, whitish suture lines and an additional ammonite [in (e)] at the apertural end of the body chamber due to the limonitic preservation and the embedding limestone in grey. Cracks through the ammonite are dark grey. The surrounding air is black.

Lower to Upper Carnian Kasimlar Formation (Julian 2–Tuvalian1, *Austrotrachyceras austriacum* Zone–*Tropites dilleri* Zone). A detailed description of the geology and lithostratigraphy is given in LUKENEDER S. et al. (2012) and LUKENEDER S. & A. LUKENEDER (2014).

The investigated Upper Triassic ammonoids are *Kasimlarcelites krystyni* LUKENEDER S. & A. LUKENEDER (family Celtitidae MOJSISOVIC; Fig. 3, 4), *Sandlingites* cf. *pilari* DIENER (family Sandlingitidae TOZER; Fig. 5) and *Trachysagenites* cf. *beckei* DIENER (family Haloritidae MOJSISOVIC; Fig. 6). All ammonoids are members of the order Ceratitida HYATT.

Cretaceous ammonoids from the Dolomites in Italy

This case differs in lithology and taphonomical features from the Triassic case study above. The same methods and equipment were used as for the Triassic samples.

This fossil cephalopod originates from the Puez locality (Dolomites, northern Italy). The material was collected within the FWF project P20018-N10 and is stored at the NHMW. Inventory numbers are given for the investigated specimens from *Lytoceras* (NHMW-2013/0569/0001) and *Dissimilites* (holotype NHMW-

2012/0002/0001). The lytoceratid ammonite *Lytoceras* was collected by Martin MASLO and the heteromorph ammonite *Dissimilites* by S. LUKENEDER from Lower Barremian beds (approx. 129 million years old) at the Puez section. The outcrop is situated on the Puez-Geisler-Gardenaccia Plateau in the Dolomites (maps Trentino – Alto Adige; South Tyrol; LUKENEDER A. 2010). The position is about 30 km northeast of Bozen (E011°49 15 N46°35 30; LUKENEDER A. 2010, 2012). The fossil cephalopods derive from the Puez Formation (Puez Limestone Member; LUKENEDER A. 2010). The ammonoids reported within this work derive from the middle part of the Puez Limestone Member with Lower Barremian sediments (*Moutoniceras moutonianum* Zone; LUKENEDER A. & S. LUKENEDER 2014). A detailed description of the geology and lithostratigraphy is given in LUKENEDER A. (2010).

The investigated Lower Cretaceous ammonoids were *Lytoceras subfimbriatum* (D'ORBIGNY) (family Lytoceratidae NEUMAYR) and *Dissimilites intermedius* LUKENEDER A. & S. LUKENEDER (family Acriceratidae VERMEULEN; Fig. 7). The ammonoids are members of the order Ammonoidea ZITTEL, and the subsequent suborders Lytoceratina HYATT and Ancyloceratina WIEDMANN.

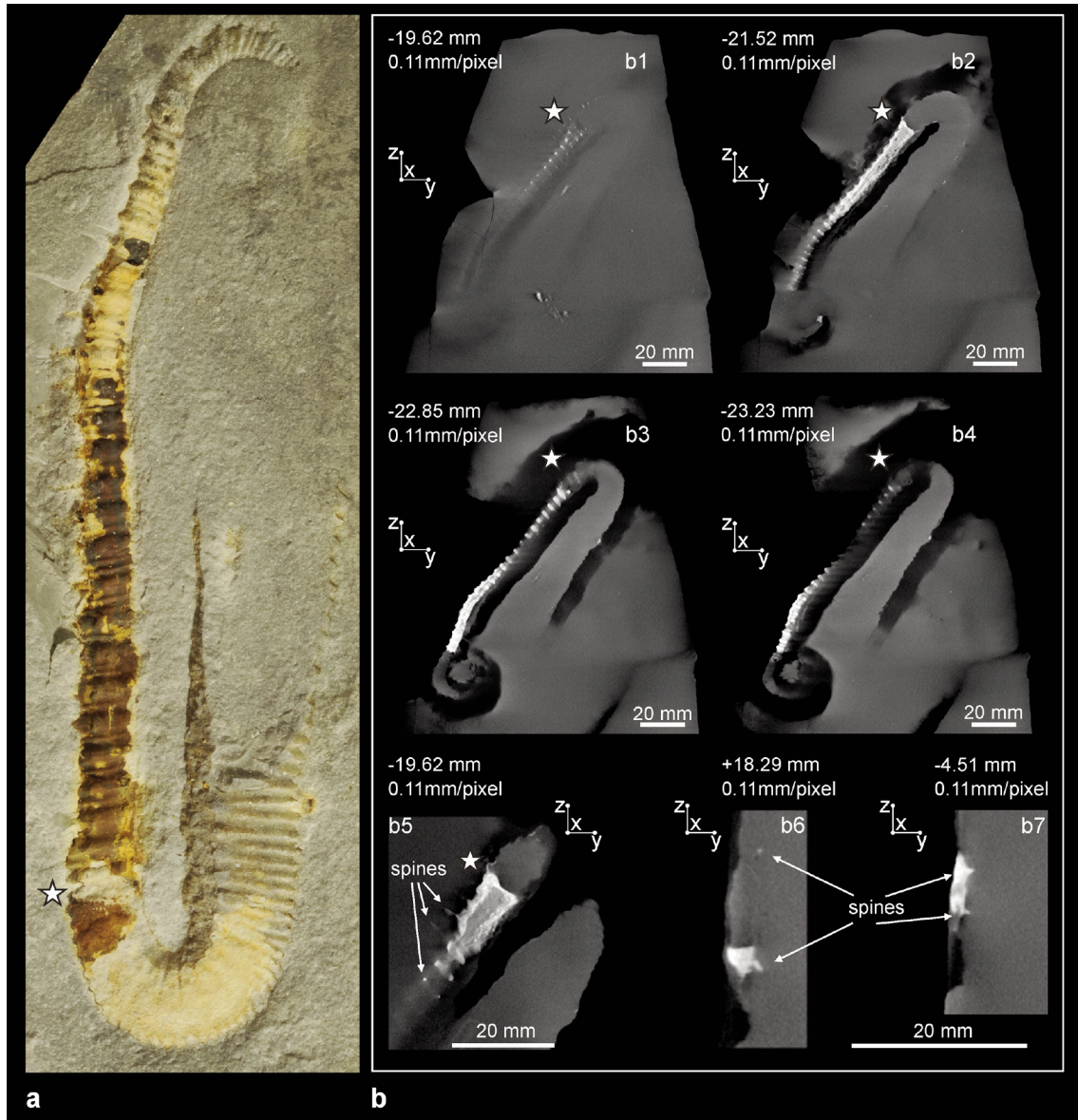


Fig. 8: *Dissimilites intermedius*. (a) Lateral view, uncoated with limonitic preservation, yellow to orange, holotype NHMW-2012/0002/0001. (b) CT frontal (b1-b5) and axial (b6-b7) view slices: (b1) CT slice 421; (b2) CT slice 441; (b3) CT slice 455; (b4) CT slice 460; (b5) detail of CT slice 797; (b6) detail of CT slice 862; (b7) detail of CT slice 622. Computed tomography slices from the specimen with limonitic preservation in white and the embedding limestone in grey. Asterisks mark the beginning of body chamber. Note the delicate spines in CT slices (b5), (b6) and (b7).

Methods, results and visualisation

Macrophotography

Detailed images of the specimens were taken with a Kodak Professional DCS Pro combined with the photo device Stereo Discovery V20 with AxioCam MR5 Zeiss. All images have the same file structure with 600 dpi resolution. Black-and-white images are combined with full colour images for high visibility of edges and details of the fossil.

Computed tomography

3D computed tomography was performed with a 225 kV microfocus and a 450 kV minifocus X-ray tube. The specimen and the embedding fossiliferous marly limestone were tomographed frontally and axially (angle of 90°; Figs 2, 3). Frontal and axial slice-images were animated to videos as motion pictures.

From the Triassic *Kasimlarceltites* (holotype, NHMW-2012/0133/0014), 320 frontal slices (0000.jpg–319.jpg; 146 MB) with 0.11 mm/pixel space were produced. The rock sample with the *Kasimlarceltites* mass-occurrence (NHMW-2013/0568/0003) appears with

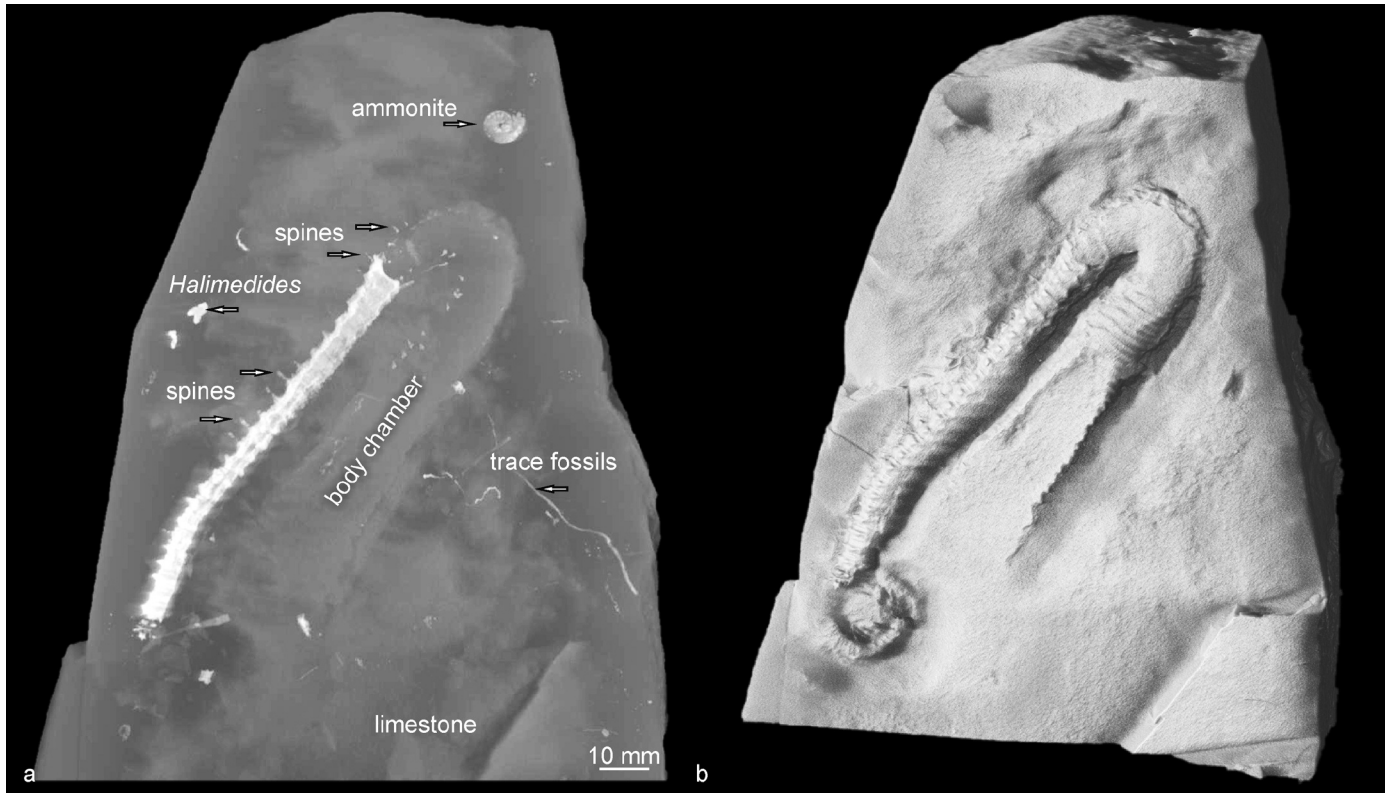


Fig. 9: Limestone rock with the holotype of *Dissimilites intermedius*, lateral view, NHMW-2012/0002/0001. (a) Maximum intensity projection with visible ammonoids and trace fossils with *Halimedes*; (b) rendered CT surface of the same specimen. Whitish suture lines and trace fossils due to the limonitic preservation and the embedding limestone in grey.

310 frontal slices (000.jpg–309.jpg; 157 MB) with 0.11 mm/pixel space and 338 axial slices (527.jpg–864.jpg, 93.3 MB) with 0.11 mm/pixel space. From *Sandlingites* 463 frontal slices (000.jpg–462.jpg; 450 MB) with 0.11 mm/pixel space were produced. From *Trachysagenites* 602 frontal slices (000.jpg–601.jpg; 388 MB) with 0.11 mm/pixel space were produced.

From the Cretaceous *Dissimilites*, 655 frontal slices (000.jpg–654.jpg; 342 MB) with 0.11 mm/pixel space and 1768 axial slices (0000.jpg–1767.jpg, 518 MB) with 0.11 mm/pixel space were produced. From *Lytoceras* 675 frontal slices (000.jpg–674.jpg; 528 MB) with 0.11 mm/pixel space were produced.

Measurements were performed with durations of 56, 68 and 92 minutes. Voxel sizes were 95 and 75.01 μm . Tube voltage was adjusted to 220 and 400 kV with 425 and 1500 A. Exposure time was 600, 999, and 2000 ms. 1440 projections with a Cu pre-filter 1.0, 2.0 and 4.0 mm were made. Additionally, the surface (e.g. stone vs. air) was rendered to image the cephalopod's morphology.

3D visualisation and motion pictures of fossil cephalopods

Studies on computed tomography and laser scans are essential for palaeontologic and systematic investi-

gations. Especially when extraction of fossils from embedding sediments is impossible, or the fossil and its delicate morphological parts (e.g. spines, ribs) would be destroyed by preparation.

Triassic ammonoid shells and filled phragmocones (both secondary calcite) from the *Kasimlarceltites* beds (LUKENEDER S. & A. LUKENEDER 2014) possess the same mass-density as the matrix (i.e. limestone) in which the ammonoid specimens are embedded. The almost identical mass-density of the various carbonates of the embedding matrix (about 2.8 g/cm³), the ammonoid shell (secondary calcite, about 2.6–2.8 g/cm³), and the infilled matrix (about 2.8 g/cm³) avoids their visualisation, especially of morphological details, via computed tomography. It is therefore not possible to visualise inner parts of the ammonoids by computed tomography (Fig. 3–5). In few cases ammonoid shells, body chambers, and secondary formed calcite fissures can be observed in computed tomographic images and movies (Fig. 4). For instance, a secondarily precipitated sparry calcite (in cleavage and cracks) is visible in the Triassic sample of the *Kasimlarceltites* beds (Fig. 4b). In contrast, hundreds of ammonoid specimens within that mass-occurrence “vanish” on CT slices. Disseminated pyrite cubes within the chambered part of the ammonoid (i.e. the phragmocone) define exactly the internal dimension and

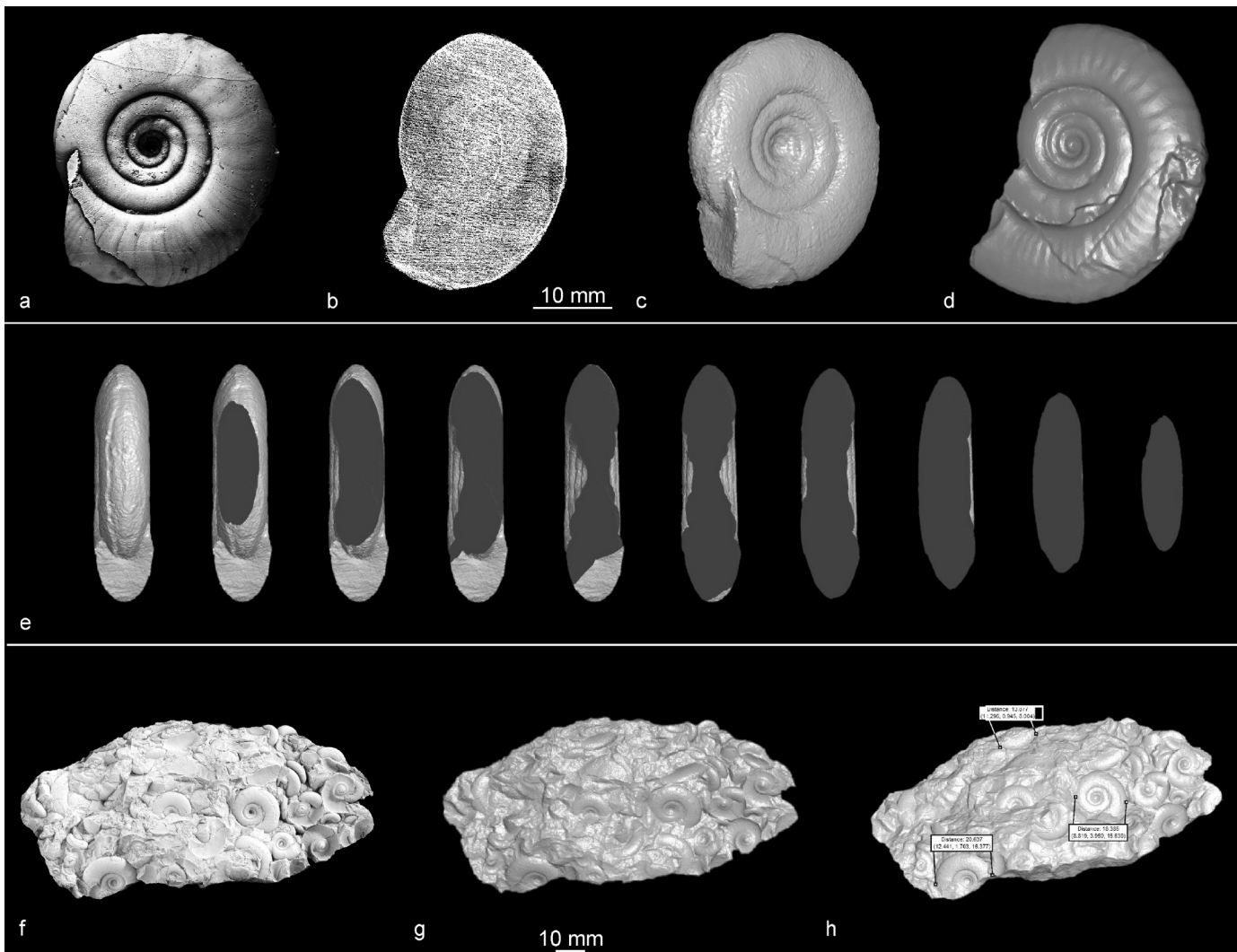


Fig. 10: *Kasimlarceltites krystyni*. (a) Lateral view, NHMW-2012/0568/0001, coated with ammonium chloride; (b) basic laser scan point cloud; (c) rendered laser scan surface; (d) rendered laser scan surface of the holotype, NHMW-20120133/0014; (e) digital slices through rendered laser scan surface; (f) rock sample of the mass-occurrence NHMW-2013/0568/0002, coated with ammonium chloride; (g) rendered laser scan surface; (h) rendered laser scan surface with dimensions of ammonoids.

shape of *Trachysagenites* (Fig. 6a–h). Future work will be done within a project on the possibilities of computed tomography in such dense Mesozoic limestones. GARWOOD et al. (2009, 2010) described two additional possibilities for using CT scans on material of similar density. These authors suggested scanning the material at low X-ray energy in order to reveal the different phases. By the use of a phase contrast holotomography at a synchrotron computed tomography device, crystal structures can be rendered visible (GARWOOD et al. 2010).

In rare cases, the investigated Cretaceous ammonoids are secondarily coated by iron sulphides as pyrite and marcasite (both FeS_2), or by hydrated iron oxide-hydroxides as limonite ($\text{FeO}(\text{OH}) \times n\text{H}_2\text{O}$). Such steinkerns or limonitic fillings are detected by CT due to the increased density of these iron compounds

(pyrite and marcasite: $4.8\text{--}5.0\text{ g/cm}^3$; limonite: $2.7\text{--}4.3\text{ g/cm}^3$). Hence, these dense structures, e.g. fine coatings on fossils or pyrite cubes, can be visualised by computed tomography without any destruction of the fossils, morphological features can be analysed in three-dimensional space, and, furthermore, internal structures can be visualised. The shape data derive from the recently described species *Dissimilites intermedius* LUKENEDER A. & S. LUKENEDER, 2014 (Fig. 8).

The main differences between the Triassic and the Cretaceous fossil material are the embedding sediments (i.e. the matrix) as well as the secondary material of ammonoid shells and penetrating trace fossils. The presence of iron sulphides and iron oxide-hydroxides within sediments or fossils increases the potential of useful computed tomography data. Surface laser scans are un-



Fig. 11: 3D reconstruction of successive ontogenetic stages in the fossil cephalopod *Dissimilites intermedius*, based on CT data (after LUKENEDER 2012). (a) cyrtocone juvenile animal; (b–d) mid-aged animal with straight shell stages; (e–h) different views of the adult, mature ammonite animal.

affected by the difference in sediments. Within marly limestones from the Lower Cretaceous numerous ammonoids from the Lower Barremian (e.g. *Lytoceras*, *Dissimilites*) and trace fossils (*Halimedes*) are preserved as secondary limonitic steinkerns or limonitic fillings. These dense structures can be visualised by computed tomography (Fig. 9). New morphological details such as spines and delicate parts on ammonite shells, the shape and position of suture lines, and the exact structure of trace fossils can be detected and visualised (Fig. 9).

The modelling procedure of the fossil cephalopods is based on a series of CT images, which turned out to be an essential source to understand the cephalopod morphology and shape. Invisible (e.g. when covered by sediment) delicate structures such as spines and suture

lines appear within CT data. The digital CT images present a grey scale spectrum which was further refined by converting its height information, ranging from darker to lighter areas, to a so-called “Normal Map” image. This helped to refine the visual appearance and understand various delicate structures. The process involved projecting this Normal Map onto a surface inside a 3D Realtime Editor, and then introducing a virtual light source (LUKENEDER A. 2012), which was tilted in different directions to gain plasticity from highlights and shadows.

The 3D modelling procedure was carried out in different stages using different 3D modelling and animation software facilities and programmes (e.g. Nurbs Realtime Editor, Model Editor or 3d Studio Max® from

Autodesk®), each specialised for its defined task. The first step was to achieve a precise volume model of the fossil cephalopod, followed by refining its geometric shape by adjusting scale and patterns to place the discrete spines. Final textures can be created by colouration and image information directly on its surface in preparation for the final rendering and animation process (LUKENEDER A. 2012; Fig. 11).

The outline of *D. intermedius* was vectorised and imported into a CAD Application (Rhinoceros® 4.0), which is orientated to create 3D geometry from so-called NURBS (Non Unified Rational B-Splines), and hereafter used as a guideline to extrude the prepared cross-sections along its edges (LUKENEDER A. 2012). Various other techniques had been tested before, including the manual extrusion of the sections or their replication, but with unsatisfactory results.

The final geometries were then re-imported to 3D Studio Max® for the animation and rendering setup (LUKENEDER A. 2012). For the animation of the animal's body, virtual "elements" were created by the inverse kinematic bones system and linked to a hierarchy with inverse kinematic constraints. This allows the animator to move several bones by using only the last link of this hierarchy.

Although the presented animation is based on the best preserved and most complete specimen known, the embryonic stage is still unknown in *Dissimilites* (LUKENEDER A. 2012; LUKENEDER A. & S. LUKENEDER 2014).

The exact position of the suture lines in *Lytoceras subfimbriatum* appears clearly in the CT- as well as in the rendered images (Fig. 7)

Conclusions

The study presents results of an object-based combined analysis from computed tomography and various computed 3D facility programmes performed on the most complete shells of fossil cephalopods from Mesozoic sediments. Upper Triassic (Carnian) ammonoids from the Taurus Mountains in Turkey and Lower Cretaceous (Barremian) species from the Southern Alps of Italy have been investigated.

Upper Triassic ammonoids are *Kasimlarceltites krystyni* LUKENEDER S. & A. LUKENEDER, *Sandlingites cf. pilari* DIENER, and *Trachysagenites cf. beckeii* DIENER. All of these are members of the order Ceratitida HYATT. Lower Cretaceous ammonoids were *Lytoceras subfimbriatum* (D'ORBIGNY) and *Dissimilites intermedius* LUKENEDER A. & S. LUKENEDER. The ammonoids are members of the order Ammonoidea ZITTEL.

The almost identical mass-density of the embedding limestone matrix (about 2.8 g/cm³), the ammonoid shell with secondary calcite (about 2.6–2.8 g/cm³), and the infilled limestone matrix (about 2.8 g/cm³) prevents the visualisation of internal parts and structures in the palaeontological material of the Upper Triassic from Turkey. Only pyrite cubes, formed in the phragmocone of a few ammonoids, passively show the morphology of the ammonoids' internal dimensions and structures (e.g. body chamber versus phragmocone).

In rare cases, especially in the Lower Cretaceous, the ammonoids are coated by iron sulphides as pyrite and marcasite (both FeS₂) or by hydrated iron oxide-hydroxides as limonite (FeO(OH) × nH₂O). Such steinkerns or limonitic fillings are detected by CT due to the increased density of these iron compounds (pyrite and marcasite: 4.8–5.0 g/cm³; limonite: 2.7–4.3 g/cm³). Dense structures as fine coatings on fossils or infillings of trace fossils can be visualised by computed tomography. Hence, pyritised or limonitic fossils bear the highest potential for high quality CT imaging and subsequent palaeontological reconstruction.

The use of computed tomography images and laser scans of fossil cephalopods from the Taurus Mountains of Turkey and the Southern Alps of Italy resulted in 3D visualisations. Moreover, computed tomography and palaeontological data were combined to produce 3D reconstructions, yielding animated clips running through CT data slices. The case studies demonstrate the non-destructive possibilities of 3D visualisation of palaeontological material. The resulting images are of high quality shots that are combined to short animated clips showing the morphology of fossils within CT slices in 3D. Another advantage is that the digital CT data, CT slices and CT clips can easily be shared amongst palaeontologists. This digital information can be discussed online and the resulting interpretation, based on the more detailed morphology, quickly be adapted.

The additional use of high-speed 3D scans with reduced random-noise obtained by efficient hyper-modulation increases the details in reconstructions and digitalisation of palaeontological material. Surfaces of ammonoids can therefore be reconstructed digitally without loss of information, and digital-slices can be created from rendered outlines without any destruction of the fossil.

Acknowledgements

This study benefited from grants of the Austrian Science Fund (FWF) within the projects P20018-N10 and P 22109-B17. The authors highly appreciate the help and support from the General Directorate of Min-

eral Research and Exploration (MTA, Turkey), and are thankful for the digging permission within the investigated area. Special thanks go to Yesim ISLAMOGLU (MTA, Ankara) for organization and guiding two field trips. We thank Alexander RATH (Vienna) for his advice with a software program to create movies of the 3D reconstructions and 3D laser scans. The authors appreciate the suggestions and comments of Björn BERNING (Linz) which improved the quality of the manuscript. Macrophotographs of natural and coated ammonoid specimens were taken by Alice SCHUMACHER (Vienna).

References

- BALANOFF A.M., NORELL M.A., GRELLET-TINNER G. & M.R. LEWIN (2008): Digital preparation of a probable neoceratopsian preserved within an egg, with comments on microstructural anatomy of ornithischian eggshells. — *Naturwissenschaften* **95**: 493-500.
- CUNNINGHAM J.A., THOMAS C.W., BENGTON S., KEARNS S.L., XIAO S., MARONE F., STAMPANONI M. & P.C.J. DONOGHUE (2012): Distinguishing geology from biology in the Ediacaran Doushantuo biota relaxes constraints on the timing of the origin of bilaterians. — *Proc. R. Soc. B, Biol. Sci.* **279**: 2369-2376. doi:10.1098/rspb.2011.2280
- DEGRANGE F.J., TAMBUSI C.P., MORENO K., WITMER L.M. & S. WROE (2010): Mechanical analysis of feeding behavior in the extinct "terror bird" *Andalgalornis steulleti* (Gruiformes: Phorusrhacidae). — *PLoS ONE* **5** (8): e11856. doi:10.1371/journal.pone.0011856
- DONG X.P., BENGTON S., GOSTLING N.J., CUNNINGHAM J.A., HARVEY T.H.P., KOUCHINSKY A., VAL'KOV A.K., REPETSKI J.E., STAMPANONI M., MARONE F. & P.C.J. DONOGHUE (2010): The anatomy, taphonomy, taxonomy and systematic affinity of *Markuelia*: Early Cambrian to Early Ordovician scali-dophorans. — *Palaeontology* **53** (6): 1291-1314.
- DONOGHUE P.C.J., BENGTON S., DONG X., GOSTLING N.J., HULDTGREN T., CUNNINGHAM J.A., YIN C., YUE Z., PENG F. & M. STAMPANONI (2006): Synchrotron X-ray tomographic microscopy of fossil embryos. — *Nature* **442**: 680-683.
- FORTUNY J., GALOBBART À. & C. DE SANTISTEBAN (2011): A new capitosaur from the Middle Triassic of Spain and the relationships within the Capitosauria. — *Acta Palaeont. Polonica* **56** (3): 553-566.
- FRIIS E.M., CRANE P.R., PEDERSEN K.R., BENGTON S., DONOGHUE P.C.J., GRIMM G.W. & M. STAMPANONI (2007): Phase-contrast X-ray microtomography links Cretaceous seeds with Gnetales and Bennettitales. — *Nature* **450**: 549-552.
- GAI Z., DONOGHUE P.C.J., ZHU M., JANVIER P. & M. STAMPANONI (2011): Fossil jawless fish from China foreshadows early jawed vertebrate anatomy. — *Nature* **476**: 324-327.
- GARWOOD R.J. (2010): Palaeontology in the digital age. Part one: breathing new life into old bones. — *Mag. Geol. Ass.* **9** (3): 18-20.
- GARWOOD R.J. (2011): Palaeontology in the digital age. Part two: computerized Carboniferous creatures. — *Mag. Geol. Ass.* **10** (2): 10-11.
- GARWOOD R.J., DUNLOP J.A. & M.D. SUTTON (2009): High-fidelity X-ray micro-tomography reconstruction of siderite-hosted Carboniferous arachnids. — *Biol. Lett.* **5**: 841-844.
- GARWOOD R.J., RAHMAN I.A. & M.D. SUTTON (2010): From clergymen to computers – the advent of virtual palaeontology. — *Geol. Today* **26** (3): 96-100.
- GASPARD D., PUTLITZ B. & L. BAUMGARTNER (2011): X-ray computed tomography – a promising tool for brachiopod shell investigations. — *Proceedings IAMG 2011 Salzburg 2011*: 518-533.
- HOFFMANN R. & S. ZACHOW (2011): Non-invasive approach to shed new light on the buoyancy business of chambered cephalopods (Mollusca). — *Proceedings IAMG 2011 Salzburg 2011*: 507-517.
- HULDTGREN T., CUNNINGHAM J.A., YIN C., STAMPANONI M., MARONE F., DONOGHUE P.C.J. & S. BENGTON (2011): Fossilized nuclei and germination structures identify Ediacaran "animal embryos" as encysting protists. — *Science* **334**: 1696-1699.
- KNOLL F., WITMER L.M., ORTEGA F., RIDGELY R.C. & D. SCHWARZ-WINGS (2012): The braincase of the basal sauropod dinosaur *Spinophorosaurus* and 3D-reconstructions of the cranial endocast and inner ear. — *PLoS ONE* **7** (1): e30060. doi:10.1371/journal.pone.0030060
- KRUTA I., LANDMAN N., ROUGET I., CECCA F. & P. TAFFOREAU (2011): The role of ammonites in the Mesozoic marine food web revealed by jaw preservation. — *Science* **331** (6013): 70-72.
- LUKENEDER A. (2010): Lithostratigraphic definition and stratotype for the Puez Formation: formalization of the Lower Cretaceous in the Dolomites (S. Tyrol, Italy). — *Austrian J. Earth Sci.* **103** (1): 138-158.
- LUKENEDER A. (2012): Computed 3D visualisation of an extinct cephalopod using computed tomographs. — *Comp. & Geosci.* **45**: 68-74.
- LUKENEDER A. & S. LUKENEDER (2014): The Barremian heteromorph ammonite *Dissimilites* from northern Italy: taxonomy and implications. — *Acta Palaeont. Polonica* **5x** (x): xxx-xxx. <http://dx.doi.org/10.4202/app.2012.0014>
- LUKENEDER A., LUKENEDER S. & C. GUSENBAUER (2012): Computed tomography in palaeontology – case studies from Triassic to Cretaceous ammonites. — In: *EGU General Assembly 2012, 22-27 April, Vienna, Austria. Geophys. Res. Abstr.* **14**: 283.
- LUKENEDER A., LUKENEDER S. & C. GUSENBAUER (2014): Computed tomography of fossils and sulphide minerals from the Mesozoic of Turkey. — *Conference on Industrial Computed Tomography ICT 2014, Wels, 2 pp.*
- LUKENEDER S. & A. LUKENEDER (2011): Methods in 3D modelling of Triassic ammonites from Turkey (Taurus, FWF P22109-B17). — *Proceedings IAMG 2011 Salzburg*: 496-505. doi:10.5242/iamg.2011.0225.
- LUKENEDER S. & A. LUKENEDER (2014): A new ammonoid fauna from the Carnian (Upper Triassic) Kasımlar Formation of the Taurus Mountains (Anatolia, Turkey). — *Palaeontology*. doi:10.1111/pala.12070
- LUKENEDER S., LUKENEDER A., HARZHAUSER M., ISLAMOGLU Y., KRZYSTYN L. & R. LEIN (2012): A delayed carbonate factory breakdown during the Tethyan-wide Carnian Pluvial Episode along the Cimmerian terranes (Taurus, Turkey). — *Facies* **58**: 279-296. doi:10.1007/s10347-011-0279-8
- LUO Z.X., KIELAN-JAWOROWSKA Z. & R.L. CIFELLI (2002): In quest for a phylogeny of Mesozoic mammals. — *Acta Palaeont. Polonica* **47**: 1-78.
- MALOOF A.C., ROSE C.V., BEACH R., SAMUELS B.M., CALMET C.C., ERWIN D.H., POIRIER G.R., YAO N. & F.J. SIMONS (2010): Possible ani-

- mal-body fossils in pre-Marinoan limestones from South Australia. — *Nature Geosci.* **3**: 653-659.
- MARSCHALLINGER R. (2001): Three-dimensional reconstruction and visualization of geological materials with IDL – examples and source code. — *Comp. & Geosci.* **27** (4): 419-426.
- MARSCHALLINGER R., HOFMANN P., DAXNER-HÖCK G. & R.A. KETCHAM (2011): Solid modeling of fossil small mammal teeth. — *Comp. & Geosci.* **37** (9): 1364-1371.
- MAYRHOFER S. & A. LUKENEDER (2010): 3D Modellierung eines Karnischen Ammoniten Massenvorkommens (Taurus, Türkei; FWF P22109 B17). — In: MARSCHALLINGER R., WANKER W. & F. ZOBL (Eds), *Beiträge zur COGeo 2010*, 12 pp. doi:10.5242/co-geo.2010.0000
- MEES F., SWENNEN R., VAN GEET M. & P. JACOBS (2003): Applications of X-ray computed tomography in the geosciences. — *Spec. Pap. Geol. Soc., London* **215**: 1-243.
- POLCYN M.J., ROGERS J.V., KOBAYASHI Y. & L.L. JACOBS (2002): Computed tomography of an anolis lizard in Dominican amber: systematic, taphonomy, biogeography, and evolutionary implications. — *Palaeont. Electr.* **5** (1): 13 pp. http://palaeo-electronica.org/paleo/2002_1/amber/issue1_02.htm
- RAYFIELD E.J., NORMAN D.B., CELESTE C. HORNER C.C., HORNER J.R., SMITH P.M., JEFFREY J., THOMASON J.J. & P. UPCHURCH (2001): Cranial design and function in a large theropod dinosaur. — *Nature* **409**: 1033-1037.
- RAYFIELD E.J., MILNER A.C. XUAN V.B. & P.G. YOUNG (2007): Functional morphology of spinosaur 'crocodile-mimic' dinosaurs. — *J. Vertebr. Paleont.* **27**: 892-901.
- ROWE T., KETCHAM R.A., DENISON C., COLBERT M., XU X. & P.J. CURRIE (2001): Forensic palaeontology - the *Archaeoraptor* forgery. — *Nature* **410**: 539-540.
- SAUPE E.E., FUENTE R.P., SELDEN P.A., DELCLOS X., TAFFOREAU P. & C. SORIANO (2012): New *Orchestina* SIMON, 1882 (Araneae: Oonopidae) from Cretaceous ambers of Spain and France: first spiders described using phase-contrast x-ray synchrotron microtomography. — *Palaeontology* **55** (1): 127-143.
- SCOTT A.C., GALTIER J., GOSTLING N.J., SMITH S.Y., COLLINSON M.E., STAMPANONI M., MARONE F., DONOGHUE P.C.J. & S. BENGTON (2009): Scanning electron microscopy and synchrotron radiation X-ray tomographic microscopy of 330 million year old charcoalfied seed fern fertile organs. — *Microsc. Microanal.* **15**: 166-173.
- TSUIHUIJI T., WATABE M., TSOGTBAATAR K., TSUBAMOTO T., BARSOLD R., SUZUKI S., LEE A.H., RIDGELY R., KAWAHARA Y. & L.M. WITMER (2011): Cranial osteology of a juvenile specimen of *Tarbosaurus bataar* (Theropoda, Tyrannosauridae) from the Nemegt Formation (Upper Cretaceous) of Bugin Tsav, Mongolia. — *J. Vertebr. Paleont.* **31** (3): 497-517.
- WITMER L.M. & R.C. RIDGELY (2009): New insights into the brain, braincase and ear region of tyrannosaurs (Dinosauria, Theropoda), with implications for sensory organization and behaviour. — *Anat. Rec.* **292**: 1266-1296.
- ZELENITSKY D.K., THERRIEN F., RIDGELY R.C., MCGEE A.R. & L.M. WITMER (2011): Evolution of olfaction in non-avian dinosaurs and birds. — *Proc. R. Soc. B, Biol. Sci.* **278**: 3625-3634.

Alexander LUKENEDER
 Natural History Museum Vienna
 Geological-Palaeontological Department
 Burgring 7
 1010 Vienna, Austria
 E-Mail: alexander.lukeneder@nhm-wien.ac.at

Susanne LUKENEDER
 Natural History Museum Vienna
 Geological-Palaeontological Department
 Burgring 7
 1010 Vienna, Austria

Christian GUSENBAUER
 University of Applied Sciences Upper Austria
 Wels Campus
 Stelzhamerstrasse 23
 4600 Wels, Austria

ZOBODAT - www.zobodat.at

Zoologisch-Botanische Datenbank/Zoological-Botanical Database

Digitale Literatur/Digital Literature

Zeitschrift/Journal: [Denisia](#)

Jahr/Year: 2014

Band/Volume: [0032](#)

Autor(en)/Author(s): Lukeneder Alexander, Lukeneder Susanne, Gusenbauer Christian

Artikel/Article: [Computed tomography and laser scanning of fossil cephalopods \(Triassic and Cretaceous\) 81-92](#)